SUPPLEMENTARY FIGURE LEGENDS

Figure S1. Cas9 Nickase-Mediated Site-Specific Mutagenesis of SNCA Exon 4. Related to Figure 1.

(A) SURVEYOR assay of Cas9 nickase-mediated cleavage at SNCA exon 4 in HEK293T, BE(2)-M17 and SH-SY5Y cells. Teal arrows = 408 bp cleavage products, red arrows = 357 bp cleavage products.

(B) Indels formed in HEK293T (HEK), BE(2)-M17 (M17) and SH-SY5Y (SH) cells by Cas9 nickase-mediated cleavage. Chart shows mutagenesis efficiency in each cell type. PAMs and sgRNA target sequences are highlighted in red and teal, respectively. A 12 nt duplicated region is indicated in bold and italic text. Base pair mutations are indicated in bold red text.

(C) qRT-PCR for total SNCA mRNA in HEK293T, BE(2)-M17 and SH-SY5Y cells. Data are represented as mean ± SEM.

(D) ELISA for SNCA protein in HEK293T, BE(2)-M17 and SH-SY5Y cells. Data are represented as mean ± SEM. *$p \leq 0.05$, **$p \leq 0.01$

Figure S2. Mutation Analysis and Quality Control of Isogenic iPSCs. Related to Figure 1.

(A) Representative sequence chromatograms from the top two putative off-target cleavage sites examined by PCR amplification and Sanger sequencing.

(B) Left panel (top to bottom): morphology of Clone 1-13 iPSCs at magnifications of 4x (scale bar = 1000 μm), 10x (scale bar = 400 μm), 20x (scale bar = 200 μm) and 40x (scale bar = 100 μm). Central panel (top to bottom): immunostaining for DAPI, Nanog, Tra-1-60 and the merged image (scale bar = 200 μm). Right panel (top to bottom): immunostaining for DAPI, Oct4 and the merged image (scale bar = 200 μm). The bottom right panel demonstrates the normal 46,XX g-banded karyotype of Clone 1-13 iPSCs.

(C) Scatterplots and corresponding correlation coefficients of the hPSC ScoreCard Ct values for each sample further demonstrate that the edited Clone 1-13 (double knockout) iPSCs remain similar in their expression of pluripotency and differentiation related genes to the NCRM-5 (control) and ND34391G (SNCA triplication) iPSCs ($r^2 = 0.94 - 0.96$).

(D) TaqMan hPSC ScoreCard analysis demonstrates that the expression of pluripotency genes and genes required for differentiation along endodermal, mesodermal and ectodermal lineages falls within the same range as the reference sample and is similar between the NCRM-5 (control), ND34391G (SNCA triplication) and Clone 1-13 (double knockout) iPSC lines.

Figure S3. Characterization of iPSC-Derived Neurons. Related to Figure 2.

(A) Left: schematic representation of neuronal differentiation protocol via an intermediate neural stem cell population.

(B) Morphology of NAS and AST iPSCs (10x magnification), NSCs (20x magnification) and neurons (20x magnification). Intracellular inclusions are highlighted in expanded view inserts by red arrows. Far right neuronal panels show α-synuclein immunostaining which demonstrated α-synuclein dense foci in the same perinuclear location as the intracellular inclusions (white arrows), also highlighted in expanded view inserts.

(C) RT-PCR evaluation of expression of markers of fate-committed neurons in NAS, AST and AST^{iso} iPSC-derived neurons.

(D) Phase contrast images demonstrating morphology of iPSC-derived neurons from AST and AST^{iso} genotypes.

(E) Heatmap showing expression of selected markers enriched in astrocytes, glia, microglia, neural precursors, neurons, oligodendrocytes, stem cells and other cell types in AST and AST^{iso} neurons. Colour shows expression level in transcripts per million (TPM) in RNAseq data, and three biological repeats of each genotype are shown.

Figure S4. Characterisation of Gene Expression in AST and AST^{iso} iPSCs and differentiated neurons by RNAseq. Related to Figure 2.

(A) Quantification of *SNCA* expression from RNAseq as transcripts per million (TPM) in iPSC and iPSC-derived neurons in AST and AST^{iso} lines.

(B) Heatmap of significant gene expression changes between AST and AST^{iso} genotypes in iPSC-derived neurons ($q<0.01$ and $FC>2$). KEGG enrichment identifies protein processing in the ER and spliceosome genes as most highly enriched in this set. Color indicates log2 fold changes.

(C) Expression of genes contained within the triplication region. The log2 fold changes in gene expression between the AST and isogenic lines are shown in both iPSCs (red) and neuronal derivatives (blue). Positive changes indicate an increased expression in AST when compared to the isogenic control. The extent of the deletion is highlighted in red. MMRN1 was excluded due to very low expression levels.

Figure S5. Transcriptional Activation of *SNCA* with dCas9-VPR in NAS Neurons Induces *IRE1a* Expression. Related to Figure 2 and 3.

(A) Co-transfection of dCas9-VPR with the TSS2-2 sgRNA in NAS neurons (VPR) induces *SNCA* mRNA expression up as measured by qRT-PCR.

(B) Analysis of the same cells for components of the three branches of the UPR shows upregulation of *IRE1a* mRNA in VPR neurons. Data are represented as mean ± SEM of three biological repeats. ***$p \leq 0.001$

Figure S6. Analysis of UPR Effectors in *SNCA* Triplication iPSC-Derived Neurons by RNA-seq and Western Blotting. Related to Figure 3.

(A) Gene expression of XBP1 targets across differentiation stage and genotype. Data of three biological replicates from RNAseq is shown as transcripts per million (TPM) in iPSC and iPSC-derived neurons in AST and AST^{iso} lines. *p ≤ 0.05, **p ≤ 0.01 and ***p ≤ 0.001

(B) Validation of protein expression level differences in terminal UPR effectors by western blotting. Levels of BCL-2 and Beclin-1 protein were evaluated by western blotting in NAS, AST and AST^{iso} iPSC-derived neurons. Images of immunoblots appear in the left panel and quantified protein levels are graphically represented in the right panel. Data are represented as mean ± SEM of biological triplicates. *p ≤ 0.05, **p ≤ 0.01 and ***p ≤ 0.001

Figure S7. Progressive Activation of the IRE1a/XBP1 Arm of the UPR During Neuronal Differentiation of iPSCs. Related to Figure 3.

UPR gene expression profiling by qRT-PCR comparing NAS and AST iPSCs, NSCs and neurons. AST iPSCs generally lack UPR activation compared to NAS iPSCs. Activation of the IRE1a/XBP1 axis of the UPR becomes evident in AST NSCs and amplified in AST neurons compared to NAS NSCs and NAS neurons, respectively. Notably, terminal UPR activation is attenuated in AST NSCs compared to AST neurons, as evidenced by the lesser induction of CHOP and BIM, and compensatory activation of BCL-2. Data are represented as mean ± SEM of three biological repeats. *p ≤ 0.05, **p ≤ 0.01 and ***p ≤ 0.001
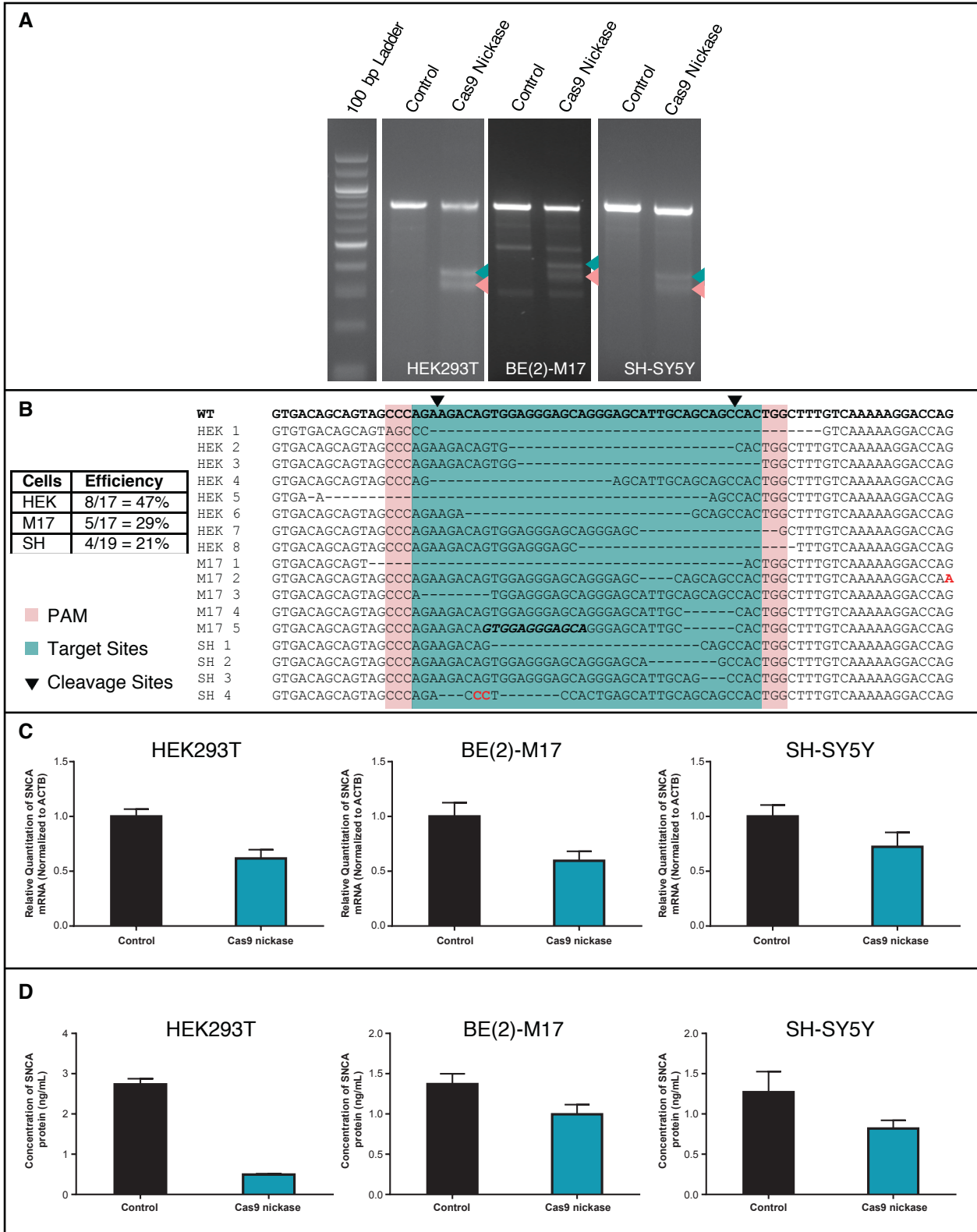
Figure S1. Cas9 Nickase-Mediated Site-Specific Mutagenesis of SNCA Exon 4. Related to Figure 1.
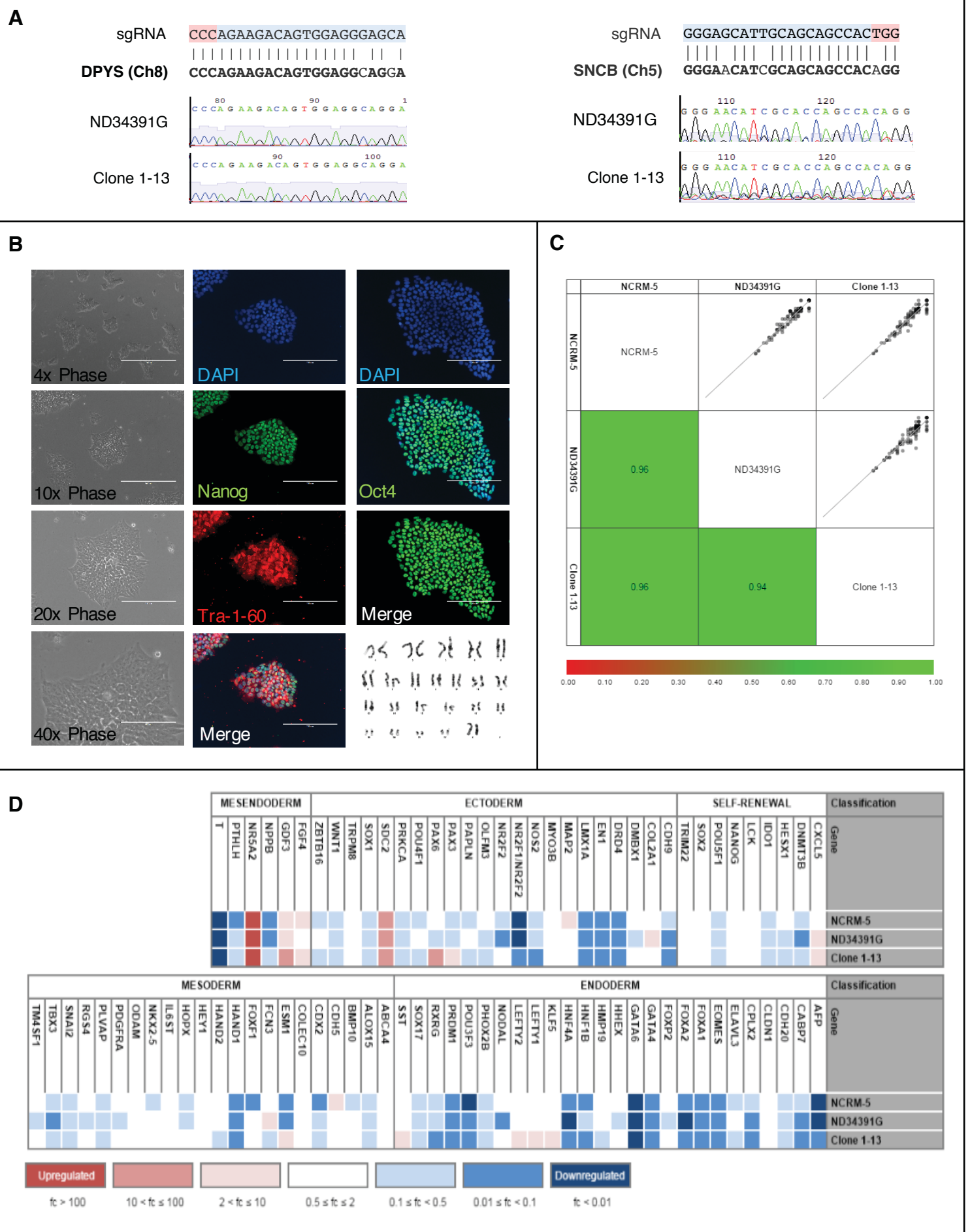
Figure S2. Mutation Analysis and Quality Control of Isogenic iPSCs. Related to Figure 1.
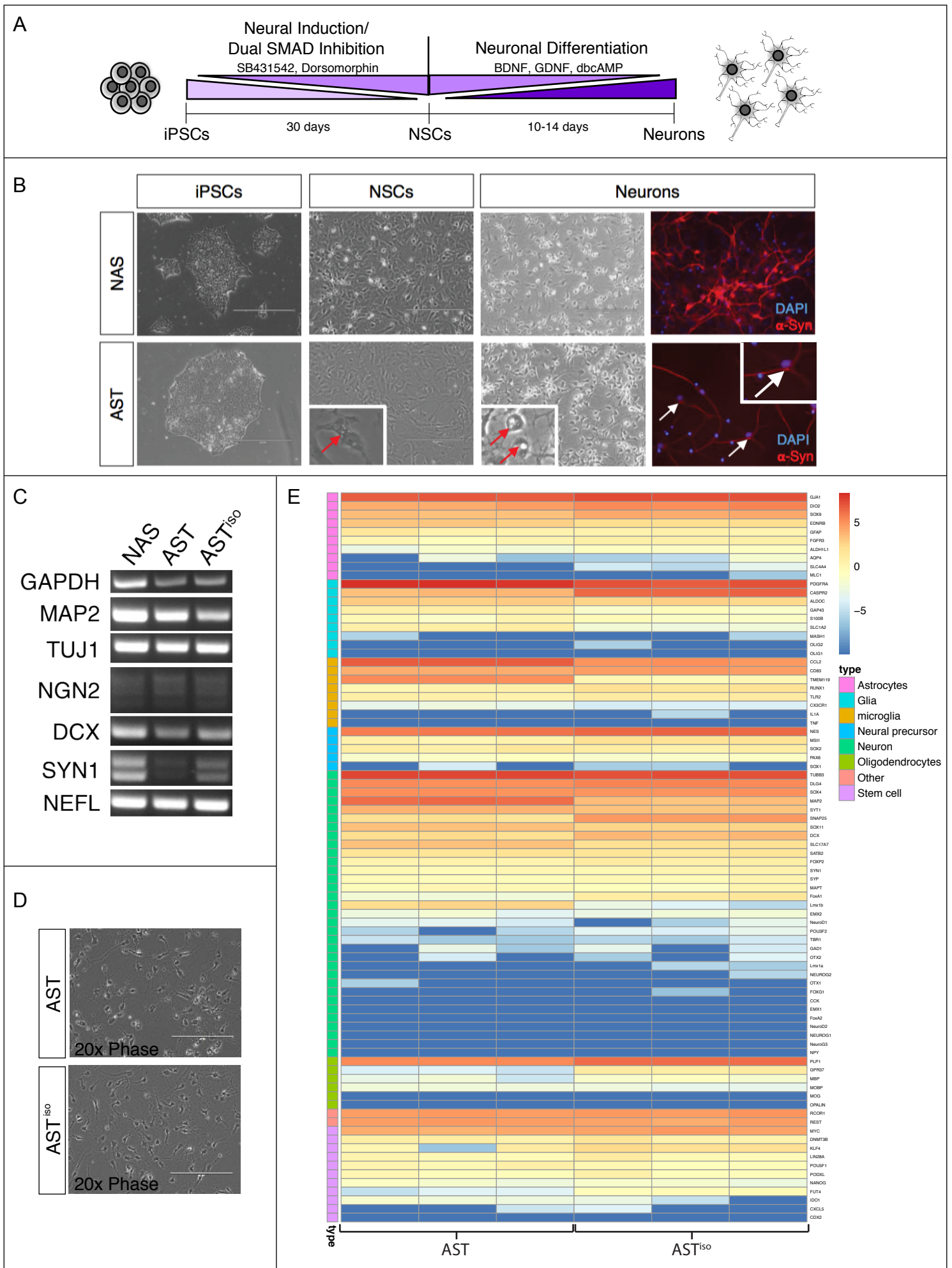
Figure S3. Characterization of iPSC-Derived Neurons. Related to Figure 2.
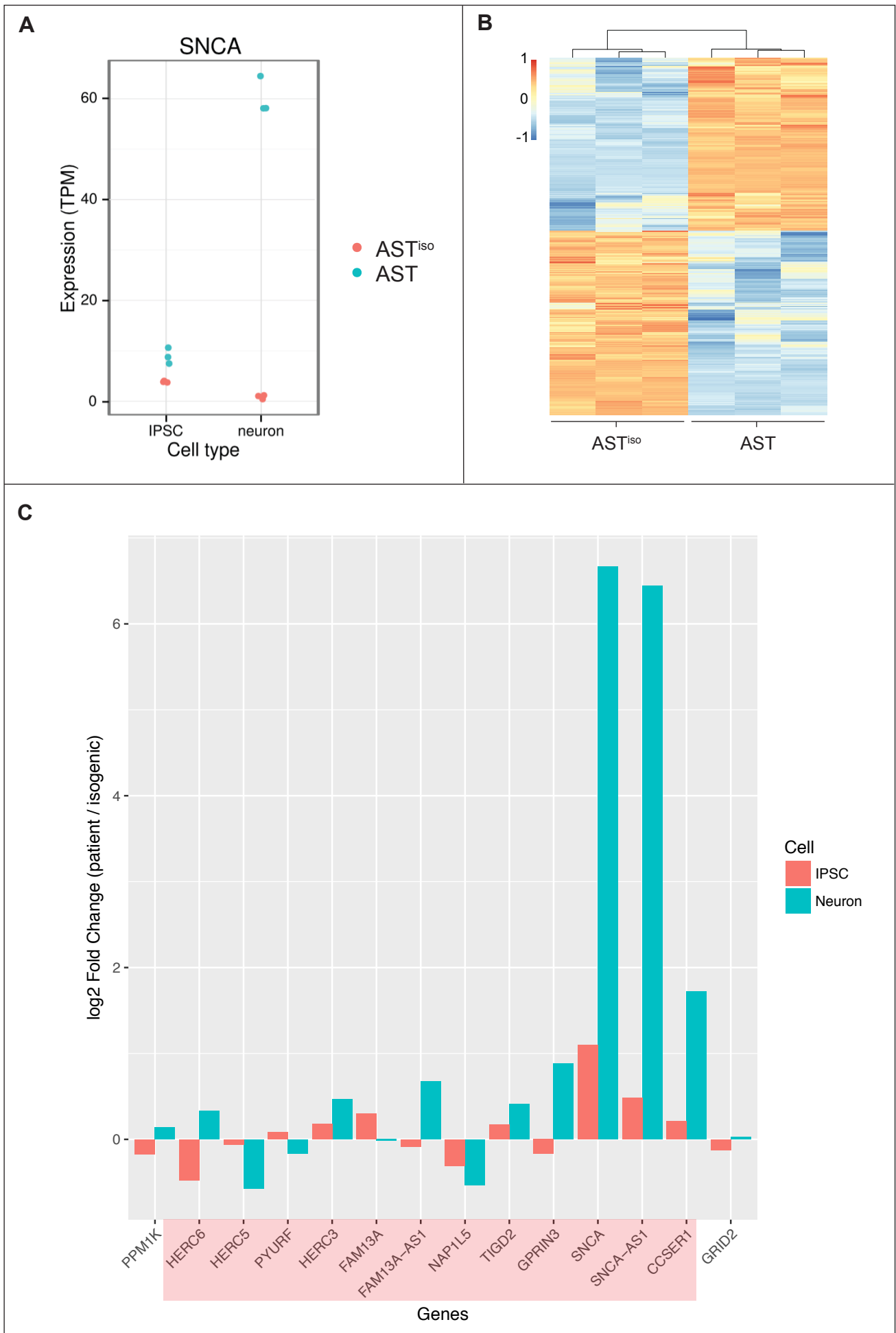
Figure S4. Characterisation of Gene Expression in AST and ASTiso iPSCs and Differentiated Neurons by RNAseq. Related to Figure 2.
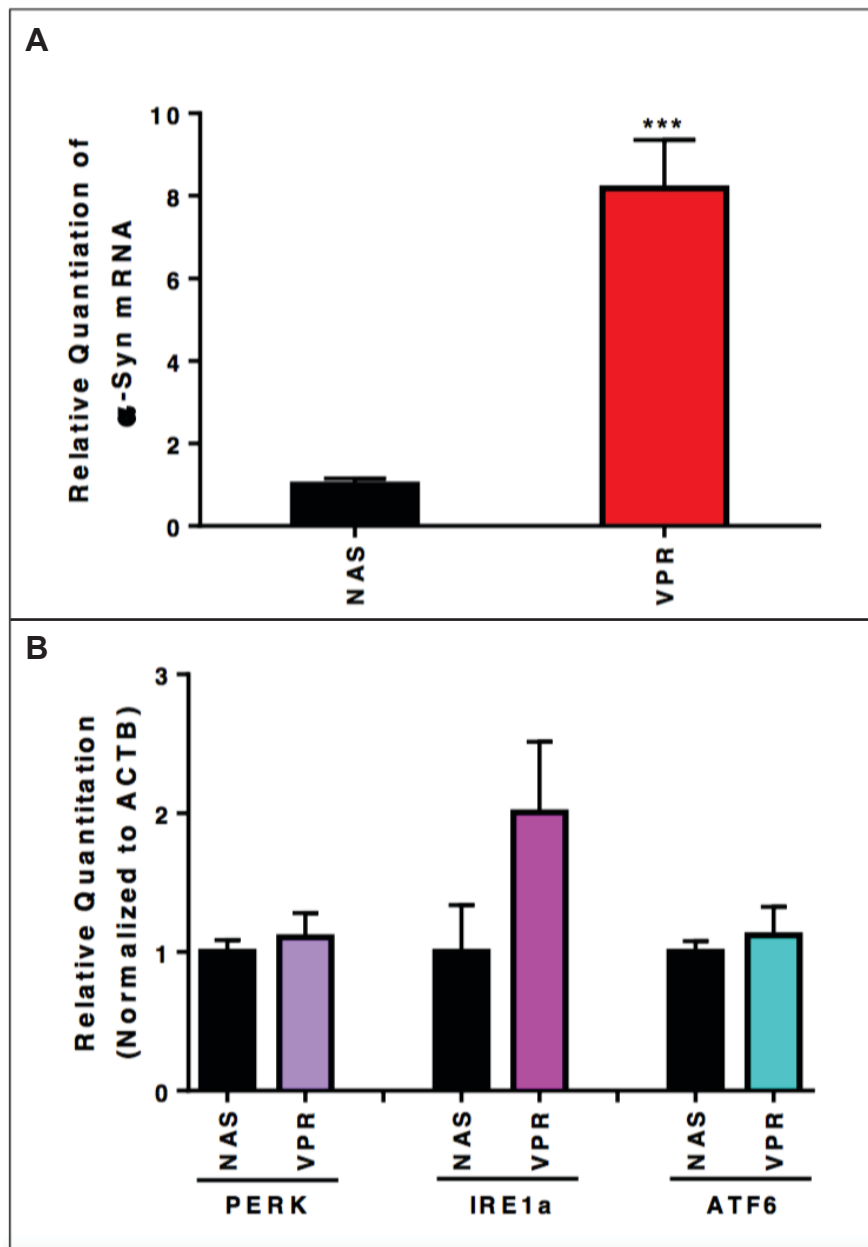
Figure S5. Transcriptional Activation of SNCA with dCas9-VPR in NAS Neurons Induces IRE1a Expression. Related to Figures 2 and 3.
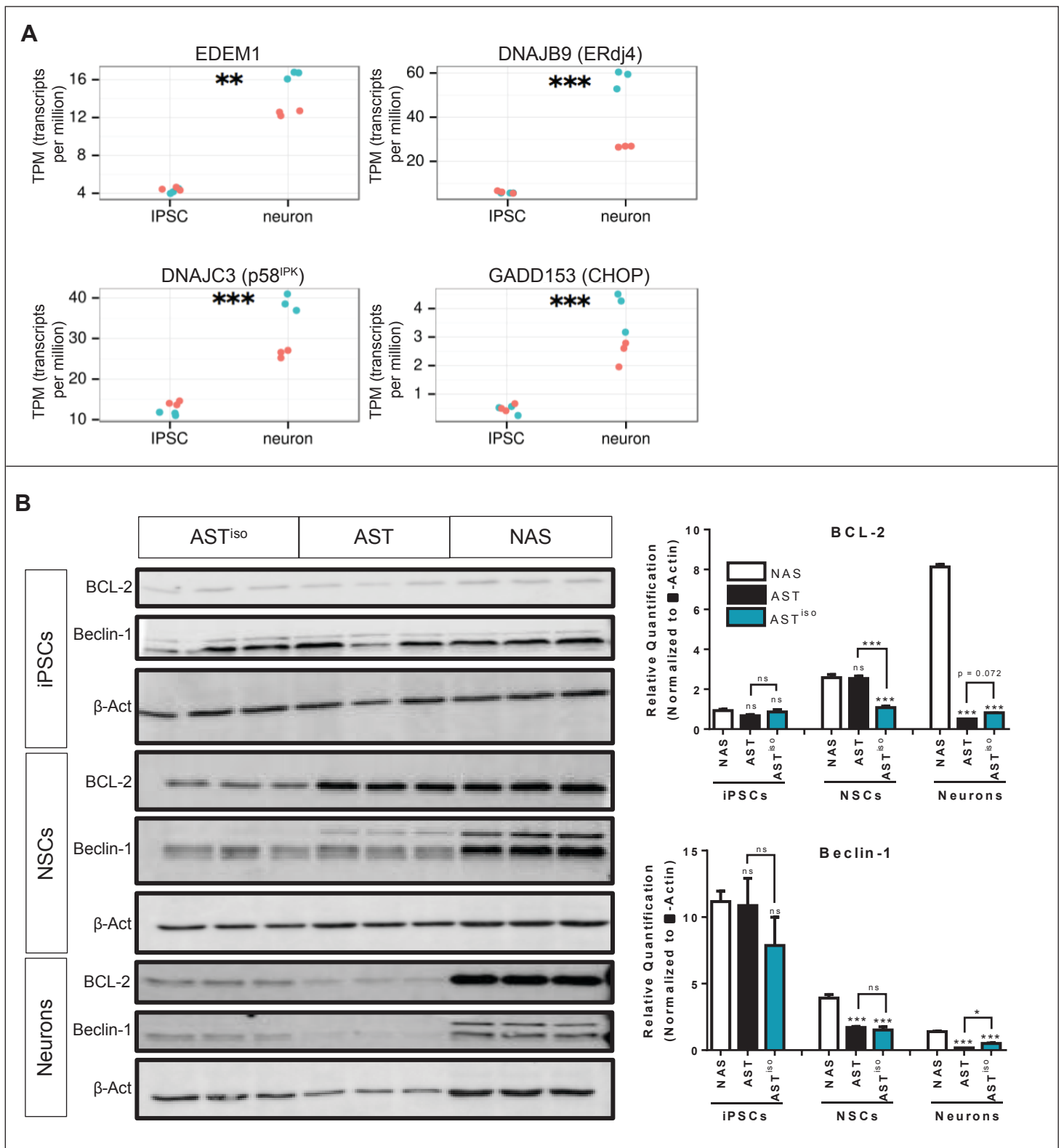
Figure S6. Analysis of UPR effectors in SNCA triplication iPSC-derived neurons by RNA-seq and Western blotting. Related to Figure 3.
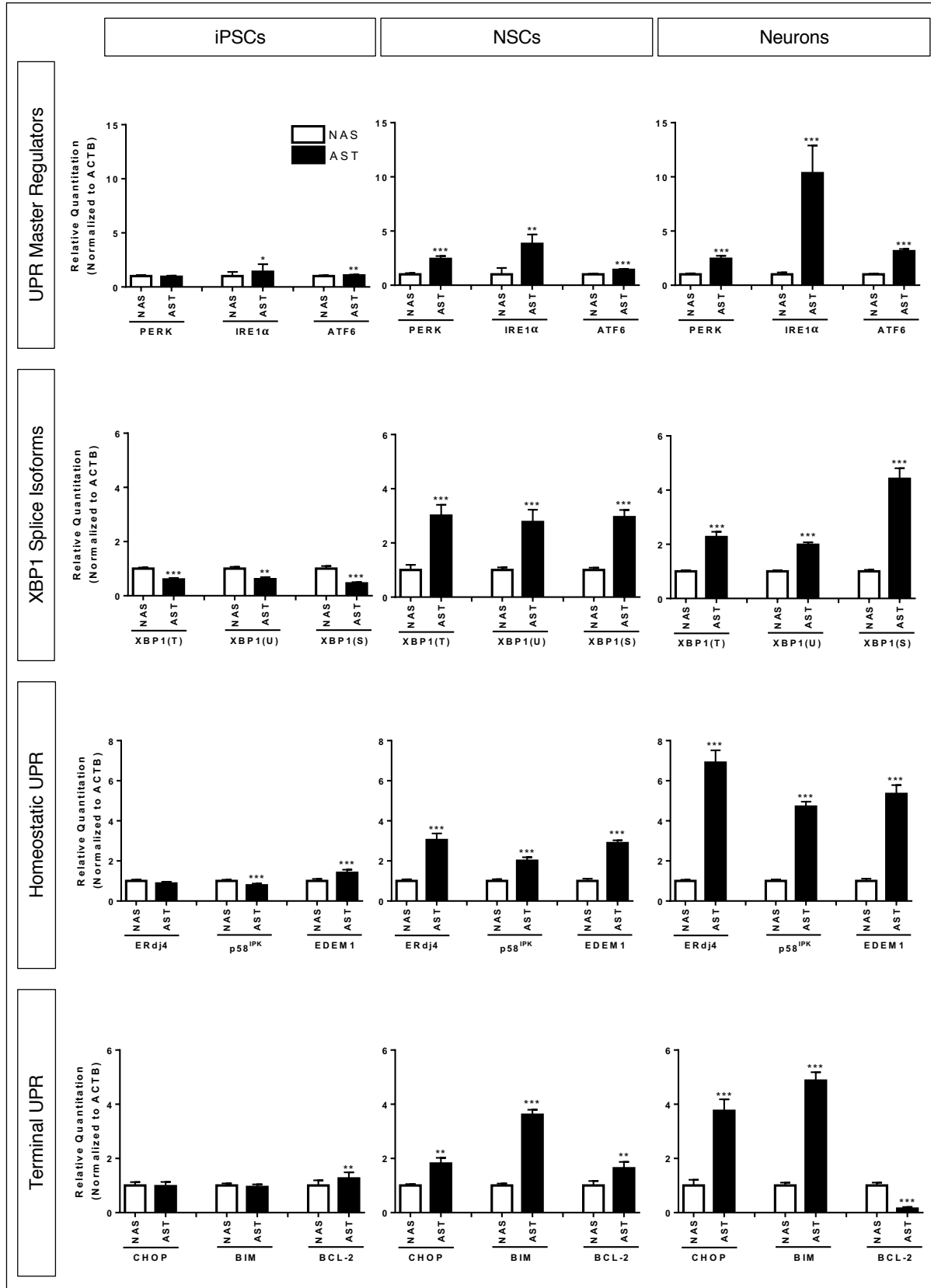
Figure S7. Progressive Activation of the IRE1α/XBP1 Arm of the UPR During Neuronal Differentiation of iPSCs. Related to Figure 3.

KEGG Term	Significance (q)
Protein processing at the ER	5.99×10^{-8}
Spliceosome	7.63×10^{-7}
Lysosomal genes	1.96×10^{-3}
N-Glycan biosynthesis	4.22×10^{-2}
Ribosome biogenesis in eukaryotes	1.64×10^{-3}
RNA transport	2.19×10^{-2}

Table S1. Top KEGG Pathways Enriched in Differentially Expressed Gene Set. Related to Figure 2.

#	category	P-value (overexpressed in patient line)	numDEInCat	numInCat	term	ontology	FDR
1110	GO:0006351	0	377	982	transcription, DNA-templated	BP	0
1114	GO:0006355	0	363	956	regulation of transcription, DNA-templated	BP	0
2132	GO:0009889	0	450	1134	regulation of biosynthetic process	BP	0
2227	GO:0010467	0	531	1285	gene expression	BP	0
2228	GO:0010468	0	446	1123	regulation of gene expression	BP	0
2258	GO:0010556	0	412	1062	regulation of macromolecule biosynthetic process	BP	0
2771	GO:0016070	0	449	1117	RNA metabolic process	BP	0
2897	GO:0018130	0	457	1133	heterocycle biosynthetic process	BP	0
2970	GO:0019219	0	426	1086	regulation of nucleobase-containing compound metabolic process	BP	0
2973	GO:0019222	0	699	1637	regulation of metabolic process	BP	0
3028	GO:0019438	0	458	1135	aromatic compound biosynthetic process	BP	0
3694	GO:0031323	0	660	1558	regulation of cellular metabolic process	BP	0
3697	GO:0031326	0	445	1118	regulation of cellular biosynthetic process	BP	0
4131	GO:0032774	0	386	997	RNA biosynthetic process	BP	0
4593	GO:0034654	0	447	1116	nucleobase-containing compound biosynthetic process	BP	0
7148	GO:0051171	0	459	1148	regulation of nitrogen compound metabolic process	BP	0
7191	GO:0051252	0	382	992	regulation of RNA metabolic process	BP	0
7713	GO:0060255	0	650	1536	regulation of macromolecule metabolic process	BP	0
9191	GO:0080090	0	654	1543	regulation of primary metabolic process	BP	0
9400	GO:0090304	0	498	1224	nucleic acid metabolic process	BP	0
9603	GO:0097659	0	380	987	nucleic acid-templated transcription	BP	0
9943	GO:1901362	0	469	1165	organic cyclic compound biosynthetic process	BP	0
10493	GO:1903506	0	366	962	regulation of nucleic acid-templated transcription	BP	0
11044	GO:2000112	0	403	1037	regulation of cellular macromolecule biosynthetic process	BP	0
11412	GO:2001141	0	367	965	regulation of RNA biosynthetic process	BP	0
5731	GO:0044271	0	520	1254	cellular nitrogen compound biosynthetic process	BP	0
1008	GO:0006139	0	595	1403	nucleobase-containing compound metabolic process	BP	0
9941	GO:1901360	0	640	1492	organic cyclic compound metabolic process	BP	0
5715	GO:0044249	0	679	1565	cellular biosynthetic process	BP	0
1879	GO:0009059	0	549	1295	macromolecule biosynthetic process	BP	0
9983	GO:1901576	0	694	1594	organic substance biosynthetic process	BP	0
6369	GO:0046483	0	618	1438	heterocycle metabolic process	BP	0
4589	GO:0034645	0	530	1253	cellular macromolecule biosynthetic process	BP	0
1351	GO:0006725	0	627	1454	cellular aromatic compound metabolic process	BP	0
1878	GO:0009058	0	707	1616	biosynthetic process	BP	0
4586	GO:0034641	0	695	1581	cellular nitrogen compound metabolic process	BP	0
6945	GO:0050794	0	1295	2735	regulation of cellular process	BP	0
5723	GO:0044260	0	970	2108	cellular macromolecule metabolic process	BP	0
1395	GO:0006807	0	781	1732	nitrogen compound metabolic process	BP	0
5708	GO:0044238	1.58E-09	1215	2572	primary metabolic process	BP	4.52E-07
5707	GO:0044237	2.57E-09	1229	2597	cellular metabolic process	BP	7.19E-07
6941	GO:0050789	3.07E-09	1370	2858	regulation of biological process	BP	8.38E-07
5453	GO:0043170	4.50E-09	1066	2272	macromolecule metabolic process	BP	1.20E-06
5919	GO:0045165	8.64E-09	17	82	cell fate commitment	BP	2.25E-06
8283	GO:0065007	1.07E-08	1453	3009	biological regulation	BP	2.74E-06
2285	GO:0010604	1.58E-08	335	792	positive regulation of macromolecule metabolic process	BP	3.95E-06
1460	GO:0006914	1.90E-08	35	129	autophagy	BP	4.63E-06
6676	GO:0048523	2.36E-08	573	1281	negative regulation of cellular process	BP	5.65E-06
6672	GO:0048519	3.34E-08	619	1373	negative regulation of biological process	BP	7.81E-06
2136	GO:0009893	4.15E-08	361	842	positive regulation of metabolic process	BP	9.52E-06
8811	GO:0071704	4.81E-08	1296	2710	organic substance metabolic process	BP	1.08E-05
1116	GO:0006357	7.61E-08	212	525	regulation of transcription from RNA polymerase II promoter	BP	1.68E-05
1123	GO:0006366	1.21E-07	228	557	transcription from RNA polymerase II promoter	BP	2.62E-05
1798	GO:0008152	1.42E-07	1349	2806	metabolic process	BP	3.02E-05
2299	GO:0010628	2.70E-07	191	474	positive regulation of gene expression	BP	5.64E-05
6187	GO:0045934	2.76E-07	146	378	negative regulation of nucleobase-containing compound metabolic process	BP	5.65E-05
6668	GO:0048513	2.88E-07	421	951	animal organ development	BP	5.79E-05
6156	GO:0045892	3.23E-07	120	320	negative regulation of transcription, DNA-templated	BP	6.40E-05
7193	GO:0051254	3.33E-07	157	399	positive regulation of RNA metabolic process	BP	6.48E-05
6157	GO:0045893	3.93E-07	150	383	positive regulation of transcription, DNA-templated	BP	7.38E-05
10495	GO:1903508	3.93E-07	150	383	positive regulation of nucleic acid-templated transcription	BP	7.38E-05
10251	GO:1902680	4.16E-07	151	385	positive regulation of RNA biosynthetic process	BP	7.70E-05
7821	GO:0060429	5.12E-07	138	355	epithelium development	BP	9.26E-05
10250	GO:1902679	5.17E-07	127	334	negative regulation of RNA biosynthetic process	BP	9.26E-05
2260	GO:0010558	5.31E-07	148	380	negative regulation of macromolecule biosynthetic process	BP	9.37E-05
10494	GO:1903507	5.88E-07	125	329	negative regulation of nucleic acid-templated transcription	BP	0.000102
3696	GO:0031325	5.97E-07	343	791	positive regulation of cellular metabolic process	BP	0.000102
1797	GO:0008150	1.11E-06	2130	4244	biological_process	BP	0.000187
7149	GO:0051172	1.25E-06	160	402	negative regulation of nitrogen compound metabolic process	BP	0.000207
3695	GO:0031324	1.30E-06	278	654	negative regulation of cellular metabolic process	BP	0.000258
2259	GO:0010557	1.60E-06	181	444	positive regulation of macromolecule biosynthetic process	BP	0.000258
11045	GO:2000113	1.91E-06	140	357	negative regulation of cellular macromolecule biosynthetic process	BP	0.000304
2200	GO:0010256	2.15E-06	61	177	endomembrane system organization	BP	0.000338
6188	GO:0045935	2.39E-06	194	470	positive regulation of nucleobase-containing compound metabolic process	BP	0.00037
2154	GO:0009987	2.44E-06	1931	3881	cellular process	BP	0.000373
6195	GO:0045944	2.48E-06	112	293	positive regulation of transcription from RNA polymerase II promoter	BP	0.000374
2135	GO:0009892	2.63E-06	300	696	negative regulation of metabolic process	BP	0.000389
7192	GO:0051253	2.64E-06	134	343	negative regulation of RNA metabolic process	BP	0.000389
3586	GO:0030855	3.45E-06	66	188	epithelial cell differentiation	BP	0.000502
2133	GO:0009890	4.41E-06	166	410	negative regulation of biosynthetic process	BP	0.000633
2286	GO:0010605	4.82E-06	272	635	negative regulation of macromolecule metabolic process	BP	0.000682

2300	GO:0010629	5.17E-06	161	398	negative regulation of gene expression	BP	0.000723
6671	GO:0048518	5.61E-06	703	1507	positive regulation of biological process	BP	0.000775
3699	GO:0031328	5.86E-06	202	483	positive regulation of cellular biosynthetic process	BP	0.000797
7150	GO:0051173	5.90E-06	210	500	positive regulation of nitrogen compound metabolic process	BP	0.000797
3698	GO:0031327	6.03E-06	163	402	negative regulation of cellular biosynthetic process	BP	0.000804
6675	GO:0048522	8.03E-06	632	1363	positive regulation of cellular process	BP	0.001059
2134	GO:0009891	8.72E-06	208	494	positive regulation of biosynthetic process	BP	0.001136
1821	GO:0008285	1.10E-05	69	192	negative regulation of cell proliferation	BP	0.001422
2131	GO:0009888	1.13E-05	248	575	tissue development	BP	0.001443
7752	GO:0060322	1.19E-05	98	254	head development	BP	0.001497
4686	GO:0035295	1.30E-05	83	222	tube development	BP	0.001622
5726	GO:0044265	1.56E-05	84	225	cellular macromolecule catabolic process	BP	0.001918
5721	GO:0044257	1.61E-05	68	189	cellular protein catabolic process	BP	0.001959
1461	GO:0006915	1.69E-05	235	550	apoptotic process	BP	0.002044
9622	GO:0098609	1.79E-05	142	347	cell-cell adhesion	BP	0.00214
2805	GO:0016236	2.82E-05	21	76	macroautophagy	BP	0.003329
3417	GO:0030154	2.95E-05	512	1108	cell differentiation	BP	0.003456
5138	GO:0042127	2.99E-05	193	459	regulation of cell proliferation	BP	0.003462
6834	GO:0048856	3.63E-05	792	1664	anatomical structure development	BP	0.004155
7121	GO:0051129	3.66E-05	74	198	negative regulation of cellular component organization	BP	0.004155
198	GO:0001709	3.87E-05	0	14	cell fate determination	BP	0.004346
3132	GO:0021537	3.91E-05	23	79	telencephalon development	BP	0.004349
2513	GO:0012501	4.02E-05	241	558	programmed cell death	BP	0.004404
1710	GO:0007420	4.03E-05	91	234	brain development	BP	0.004404
1272	GO:0006605	4.33E-05	59	164	protein targeting	BP	0.004687
1666	GO:0007275	5.41E-05	707	1492	multicellular organism development	BP	0.005803
5782	GO:0044702	6.76E-05	129	316	single organism reproductive process	BP	0.007176
7333	GO:0051603	7.93E-05	63	172	proteolysis involved in cellular protein catabolic process	BP	0.008347
6697	GO:0048565	8.19E-05	10	44	digestive tract development	BP	0.008542
1815	GO:0008219	8.28E-05	257	587	cell death	BP	0.008557
4007	GO:0032502	8.48E-05	840	1753	developmental process	BP	0.008609
3970	GO:0032436	8.48E-05	3	24	positive regulation of proteasomal ubiquitin-dependent protein catabolic process	BP	0.008609
7585	GO:0055123	9.23E-05	12	49	digestive system development	BP	0.009289
4338	GO:0033365	0.00010126	80	208	protein localization to organelle	BP	0.010099
6713	GO:0048608	0.000113789	51	142	reproductive structure development	BP	0.011154
8218	GO:0061458	0.000113789	51	142	reproductive system development	BP	0.011154
5425	GO:0043069	0.000117431	103	259	negative regulation of programmed cell death	BP	0.011414
7220	GO:0051301	0.000121035	52	145	cell division	BP	0.011665
1504	GO:0006996	0.000123788	383	841	organelle organization	BP	0.011831
2130	GO:0009887	0.000129601	146	347	animal organ morphogenesis	BP	0.01226
1200	GO:0006511	0.000130416	52	145	ubiquitin-dependent protein catabolic process	BP	0.01226
8523	GO:0070887	0.00013731	366	807	cellular response to chemical stimulus	BP	0.012803
5422	GO:0043066	0.000140455	101	254	negative regulation of apoptotic process	BP	0.012991
1819	GO:0008283	0.000143262	247	563	cell proliferation	BP	0.013145
7791	GO:0060389	0.000154716	5	29	pathway-restricted SMAD protein phosphorylation	BP	0.013952
7795	GO:0060393	0.000154716	5	29	regulation of pathway-restricted SMAD protein phosphorylation	BP	0.013952
2265	GO:0010563	0.000156932	75	195	negative regulation of phosphorus metabolic process	BP	0.013952
6189	GO:0045936	0.000156932	75	195	negative regulation of phosphate metabolic process	BP	0.013952
30	GO:0000122	0.000159042	86	220	negative regulation of transcription from RNA polymerase II promoter	BP	0.014031
3968	GO:0032434	0.000174849	6	32	regulation of proteasomal ubiquitin-dependent protein catabolic process	BP	0.015046
3106	GO:0019941	0.000175094	55	151	modification-dependent protein catabolic process	BP	0.015046
5629	GO:0043632	0.000175094	55	151	modification-dependent macromolecule catabolic process	BP	0.015046
6785	GO:0048731	0.000175795	638	1345	system development	BP	0.015046
2146	GO:0009952	0.000180832	21	71	anterior/posterior pattern specification	BP	0.015265
3598	GO:0030900	0.000181018	44	124	forebrain development	BP	0.015265
3421	GO:0030163	0.000188203	88	224	protein catabolic process	BP	0.015715
2	GO:0000003	0.000189087	146	348	reproduction	BP	0.015715
8844	GO:0071840	0.000198339	808	1685	cellular component organization or biogenesis	BP	0.016365
7140	GO:0051155	0.000201379	1	16	positive regulation of striated muscle cell differentiation	BP	0.016497
5164	GO:0042221	0.000226597	517	1109	response to chemical	BP	0.018365
8150	GO:0061180	0.000227384	2	19	mammary gland epithelium development	BP	0.018365
3347	GO:0022414	0.000229118	146	347	reproductive process	BP	0.018376
2759	GO:0016043	0.000240293	796	1659	cellular component organization	BP	0.019138
5391	GO:0042981	0.000249105	191	443	regulation of apoptotic process	BP	0.019703
5804	GO:0044767	0.000283385	829	1721	single-organism developmental process	BP	0.022261
6842	GO:0048869	0.000291721	568	1203	cellular developmental process	BP	0.02276
1877	GO:0009057	0.000299774	122	295	macromolecule catabolic process	BP	0.023128
2144	GO:0009948	0.000300475	3	22	anterior/posterior axis specification	BP	0.023128
5423	GO:0043067	0.00031164	194	448	regulation of programmed cell death	BP	0.023828
8373	GO:0070306	0.000335603	0	11	lens fiber cell differentiation	BP	0.02549
1593	GO:0007167	0.000377664	144	338	enzyme linked receptor protein signaling pathway	BP	0.028496
121	GO:0000910	0.000419002	7	33	cytokinesis	BP	0.030899
1539	GO:0007049	0.000419668	188	433	cell cycle	BP	0.030899
5761	GO:0044403	0.00042028	104	256	symbiosis, encompassing mutualism through parasitism	BP	0.030899
5767	GO:0044419	0.00042028	104	256	interspecies interaction between organisms	BP	0.030899
2116	GO:0009790	0.000423312	131	310	embryo development	BP	0.030923
2235	GO:0010506	0.000428396	27	83	regulation of autophagy	BP	0.031097
389	GO:0002088	0.000447232	3	21	lens development in camera-type eye	BP	0.03226
7106	GO:0051098	0.000450823	29	88	regulation of binding	BP	0.032265
3409	GO:0030099	0.000456918	33	96	myeloid cell differentiation	BP	0.032265
6783	GO:0048729	0.000458186	87	216	tissue morphogenesis	BP	0.032265
567	GO:0002573	0.000458554	17	58	myeloid leukocyte differentiation	BP	0.032265
10038	GO:1901800	0.000482943	5	27	positive regulation of proteasomal protein catabolic process	BP	0.033774

1443	GO:0006891	0.000506064	0	10	intra-Golgi vesicle-mediated transport	BP	0.035046
7887	GO:0060548	0.000507249	113	274	negative regulation of cell death	BP	0.035046
2756	GO:0016032	0.000558437	101	248	viral process	BP	0.038352
1708	GO:0007417	0.000562849	140	327	central nervous system development	BP	0.038424
8473	GO:0070647	0.000583966	100	245	protein modification by small protein conjugation or removal	BP	0.039617
8666	GO:0071363	0.000591838	91	223	cellular response to growth factor stimulus	BP	0.039617
731	GO:0003006	0.000592915	80	200	developmental process involved in reproduction	BP	0.039617
8131	GO:0061136	0.000594138	11	43	regulation of proteasomal protein catabolic process	BP	0.039617
3726	GO:0031399	0.000663729	219	494	regulation of protein modification process	BP	0.044002
3137	GO:0021543	0.000686507	16	55	pallium development	BP	0.04525
9141	GO:0072594	0.000713649	56	148	establishment of protein localization to organelle	BP	0.046771
5408	GO:0043010	0.000734659	29	84	camera-type eye development	BP	0.047674
2165	GO:0010033	0.000735752	397	858	response to organic substance	BP	0.047674
11469	Other	1	227	360	NA	NA	1

Cell death (especially autophagy / apoptosis)
Metabolism (especially catabolic processes)
Transcription, differentiation, cell fate

Table S2. Top GO Biological Processes Enriched in Differentially Expressed Gene Set. Related to Figure 2.

Case#	Clinical Diagnosis	Gender	Age	PMD (hrs)	Cause of Death	Immunoreactivity Score	
						Alpha-synuclein	pIRE1α
1	PD	M	82	19	PD/pneumonia	2	1
2	PD	M	77	24	PD/pneumonia	2	1
3	PD	M	74	24	PD	2	1
4	PD	M	77	48	PD/pneumonia/ lung tumor	1	1
5	PD	M	84	24	PD	2	1
6	Control	F	61	7	Cardiac infarct	0	0
7	Control	M	66	8	Aortic rupture	0	0
8	Control	M	66	24	Cardiac infarct	0	0
9	Control	M	77	24	Bradycardia	0	0
10	Control	M	67	24	Cardiac infarct	0	0
11	Control	F	73	7	Respiratory failure	0	0

Table S3. Patient Characteristics. Related to Figure 4.
PMD = post-mortem delay

Name	Forward Primer	Reverse Primer
SNCA Exon 4 Cas9 Nickase sgRNA 1	CACCGTGCTCCCTCCACTGTCTTCT	AAACAGAAGACAGTGGAGGGAGCAC
SNCA Exon 4 Cas9 Nickase sgRNA 2	CACCGGGAGCATTGCAGCAGCCAC	AAACGTGGCTGCTGCAATGCTCCC
SURVEYOR Assay	TGGCTTTACATTCCTGATCG	GGCACAAAGGGATTTGTTAC
HRM Analysis	GAGCAAGTGACAAATGTTGGAGG	CACAAAACGTACACAGCCATACC
DPYS (Ch8) RT-PCR/Sequencing	ATCAACCTGTACAGCATGCT	CTCCCTGCCCTAAAACTCCA
SNCB (Ch5) RT-PCR/Sequencing	GGATACTACAAGGCAGGGCA	TCTGAGCTGAGTCTAGCACG
GAPDH RT-PCR*	ACCACAGTCCATGCCATCAG	TCCACCACCCTGTTGCTGTA
MAP2 RT-PCR	CCTTCCTCCATTCTCCCTCC	TCCTGGGATAGCTAGGGGTT
TUJ1 RT-PCR	TGGACATCTCTTCAGGCCTG	ATGATGCGGTCGGGATACTC
NGN2 RT-PCR	CAGGCCAAAGTCACAGCAAC	GGCTCCTCCTCCTCTTCTTC
DCX RT-PCR	ATTGCCTGTGGTCCTGAAAA	CATAGGACCAGGGCTCTTGG
SYN1 RT-PCR	ACGTCCCAAACCACAGCT	GAGTGGGGTATCAGTCGGAG
NEFL RT-PCR	AGACCCTGGAAATCGAAGCA	TCACGTTGAGGAGGTCTTGG
ACTB qRT-PCR	CACAGAGCCTCGCCTTTG	GCGGCGATATCATCATCCAT
SNCA qRT-PCR	CCTTCTGCCTTTCCACCCT	TCCCTCCTTGGCCTTTGAAA
PERK qRT-PCR	ACGATGAGACAGAGTTGCGA	ATGACACCAAGGAACCGGAT
IRE1a qRT-PCR	CCGTCCTCTGTCCGTACC	GGTTTCAGGAAGCGTCACTG
ATF6 qRT-PCR	GGACTCTTTCACAGGCTGGA	CGTCTCATTTGCTGCTTCCA
XBP1 (T) qRT-PCR	AATGAAGTGAGGCCAGTGGC	ATACCGCCAGAATCCATGGG
XBP1 (U) qRT-PCR	GCACTCAGACTACGTGCACC	ATACCGCCAGAATCCATGGG
XBP1 (S) qRT-PCR	TGCTGAGTCCGCAGCAGGTG	ATACCGCCAGAATCCATGGG
ERdj4 qRT-PCR	GCAGTAGTCGGAGGGTGC	CGCTCTGATGCCGATTTTGG
p58[IPK] qRT-PCR	CTGGTGGATCTGCAGTACGA	TGTCCAGCTGCAAGTAATTTCT
EDEM1 qRT-PCR	TGACTCTTGTTGATGCATTGGA	AGACTTGGACGGTGGAATCT
CHOP qRT-PCR	GCGACAGAGCCAAAATCAGA	TGCTTTCAGGTGTGGTGATG
BIM qRT-PCR	AGTTCTGAGTGTGACCGAGA	TTGTGGCTCTGTCTGTAGGG
BCL-2 qRT-PCR	CTTGACAGAGGATCATGCTGT	TCGGATCTTTATTTCATGAGGCA

Table S4. Oligonucleotide Sequences. Related to Figures 1, 3, S1, S2, S3, S5, S7
*From Applied StemCell

SUPPLEMENTARY MATERIALS AND METHODS

iPSC Culture and Transfection

NCRM-5 (normal alpha-synuclein = NAS) healthy control iPSCs were obtained from the NIH Center for Regenerative Medicine and are distributed through RUDCR Infinite Biologics at Rutgers University. ND34391G (alpha-synuclein triplication = AST) PD patient-derived iPSCs were obtained from the Coriell Institute and are distributed through the NINDS Repository Fibroblasts and iPSCs Collection. Clone 1-13 (AST isogenic = AST^{iso}) iPSCs were generated in this study. All iPSCs were maintained under feeder-free culture conditions on BD Matrigel Matrix Growth Factor Reduced (BD Biosciences)-coated tissue culture dishes in Essential 8 (E8) medium (Life Technologies), with 100% daily medium replacement. Cells were passaged when reaching 70% confluence with a solution of 0.5 mM EDTA (Life Technologies) diluted in calcium- and magnesium-free DPBS (Life Technologies). Cells were seeded at a subcultivation ration of 1:6 to 1:24 and supplemented with 10 μM ROCK inhibitor (Y27632; Tocris Bioscience) for the first 24 hours after passaging.

To generate AST^{iso} iPSCs, AST iPSCs were transfected with the Neon Transfection System 10 μL Kit (Life Technologies). Two hours prior to transfection, 100% E8 medium containing 10 μM ROCK inhibitor was replaced on iPSCs. Cells were subsequently dissociated to a single-cell suspension with StemPro Accutase Cell Dissociation Reagent (Life Technologies) treatment and gentle trituration with a 1000 μL pipette tip. Accutase was quenched with 5 volumes of E8 medium. Cells were counted, distributed at a density of 1 x 10^6 cells per 15 mL conical tube, and pelleted by centrifugation at 200 x g for 2 min at room temperature. Cells were then washed in 3 mL PBS and re-pelleted. Equivalent amounts of each SNCA exon 4 Cas9 nickase plasmid (1 μg sgRNA1, 1μg sgRNA2) were distributed to separate tubes for each transfection reaction, totaling 2 μg of DNA per tube. Washed cells were resuspended in 10 μL Resuspension Buffer R and transferred to tubes containing DNA. The DNA and cell mixture was then electroporated using default system settings (1,400 V, 20 ms, 1 pulse) via aspiration into the 10 μL Neon tip. Cells were dispensed directly into CF-1 (GlobalStem) MEF-coated tissue culture vessels containing pre-equilibrated (37°C, 5% CO$_2$) E8 medium with 10 μM ROCK inhibitor for the first 24 hours. On the day after transfection, cell debris was gently removed by washing with DPBS, and 100% E8 medium was replaced. Cells were expanded and adapted to feeder-free culture as described in Experimental Procedures and above.

Mutation Detection by High Resolution Melt (HRM) Analysis, SURVEYOR Assay and Sanger Sequencing

For HRM analysis, HRM master mix was generated, consisting of 10 μL MeltDoctor HRM Master Mix (Life Technologies), 1.2 μL (5 μM) forward primer (Table S3), 1.2 μL (5 μM) reverse primer (Table S3) and 6.6 μL nuclease-free water for a volume of 19 μL per reaction. Genomic DNA was extracted from iPSC clones using the DNEasy Blood and Tissue Kit (Qiagen). Samples were diluted to 20 ng/μL and 1 μL of template was added to each well for a final reaction volume of 20 μL. Genomic DNA extracted from AST iPSCs was run as the reference sample. Samples were run in duplicate and the experiment was repeated, with the same four clones identified as variants. Cycling was performed on a 7500 Fast System (Life Technologies) with the following program: 95°C for 10 min, 40 cycles of 95°C for 15 sec and 60°C for 1 min, followed by the high resolution melt curve program, 95°C for 10 sec (100%), 60°C for 1 min (100%), 95°C for 15 sec (1%), 60°C for 15 sec (100%). High Resolution Melt Analysis

Software (Applied Biosystems) was used for data analysis to call variants.

Clones identified as variants by HRM were further analyzed by SURVEYOR assay. For SURVEYOR assay, the targeted region was amplified with Pfu polymerase and SURVEYOR assay primers (Table S3), followed by heteroduplex formation and SURVEYOR nuclease (Transgenomic) digestion. Cleavage products were visualized on a 2% agarose gel with 1X GelRed (Biotium).

For sequencing, PCR products were cloned into ZeroBlunt pCR vector (LifeTechnologies) and transformed into TOP10 E. coli (Life Technologies). DNA was amplified by colony PCR with the SURVYEOR assay primers and ExoSAP-IT (Affymetrix)-purified DNA was sequenced with the PCR forward primer.

iPSC Quality Control

AST[iso] iPSCs were quality controlled by karyotyping, immunofluorescence (IF) detection of pluripotency markers and TaqMan hPSC ScoreCard analysis (Life Technologies). G-band karyotyping was performed by the Cytogenetics

Laboratory at Cambridge University Hospitals. IF was performed as follows: cells were fixed in a solution of 4% paraformaldehyde diluted in PBS for 15 minutes, washed 3 times for 5 minutes in PBS, blocked in a solution of 0.3% Triton X-100 and 5% goat serum diluted in PBS, incubated in primary antibody overnight at 4°C in a solution of 0.3% Triton X-100 and 1% BSA diluted in PBS, washed 3 times for 5 minutes with PBS, incubated in secondary antibody for 3 hours, washed 3 times for 5 minutes with PBS and mounted with Vectashield HardSet Mounting Medium with DAPI (Vector Laboratories). Images were acquired using an EVOS FL Imaging System (Life Technologies). The following antibodies were used for pluripotency immunostaining: Nanog (PeproTech, 500-P236), Tra-1-60 (Millipore, MAB4360), Oct4 (Cell Signaling, 2750), goat anti-rabbit IgG Alexa Fluor 488 (Life Technologies, A-11034) and goat anti-mouse IgM 555 (Life Technologies, A-21426). TaqMan hPSC ScoreCard analysis was performed according to the manufacturer's instructions. Briefly, 20 μL of cDNA from 1 μg of RNA was diluted in 610 μL of nuclease-free water. Subsequently, 630 μL of 2X TaqMan Fast Advanced Master Mix was added, and 10 μL of the reaction mixture was loaded per well into the plate, using a fresh tip for each well. Cycling was performed on a StepOnePlus Real-Time PCR System (Life Technologies) under fast cycling conditions with the following program: 50°C for 2 min, 95°C for 20 sec and 40 cycles of 95°C for 1 sec and 60°C for 20 sec. Data were analyzed using hPSC ScoreCard Analysis Software (Life Technologies).

Derivation, Maintenance and Neuronal Differentiation of iPSC-Derived NSCs

The derivation and maintenance of NSCs from NAS and AST iPSCs was previously described (Heman-Ackah et al. 2016). Importantly, to reduce the possibility of introducing experimental variability during neural induction, we used the NSC Generation Service from Applied StemCell to generate AST[iso] iPSCs via the Chambers protocol (Chambers et al., 2009), in the same manner as AST NSCs. Like AST NSCs, AST[iso] NSCs were maintained on Geltrex LDEV-Free Reduced Growth Factor Basement membrane Matrix (Life Technologies) in Applied StemCell NSC Expansion Medium, containing 1:1 Neurobasal (Life Technologies) and DMEM/F-12 (11320-033, Life Technologies), 1X B27 supplement (Life Technologies), 1X N2 supplement (Life Technologies), 1X GlutaMax (Life Technologies) and 20 ng/mL bFGF (Peprotech). NSCs were passaged at a subcultivation ration of 1:3 to 1:6 with Accutase, and quenched

with 5 volumes of culture medium per 1 volume of Accutase.

Two days prior to seeding NSCs for neuronal differentiation, tissue culture vessels were coated with a solution of 0.01% poly-L-ornithine (Sigma-Aldrich) diluted 1:5 in culture grade water (Life Technologies). After 24 hours, poly-L-ornithine was aspirated and tissue culture vessels were rinsed twice with culture grade water before the application of 10 μg/mL laminin (Life Technologies). On the day of seeding (day 0), laminin was aspirated from tissue culture vessels and cells were seeded at a density of 1 x 10^5 NSCs per cm^2. On day 1, 100% medium was replaced with Neuronal Differentiation Medium (NDM) consisting of Neurobasal, 1X B27 supplement, 1X GlutaMax, 20 ng/mL BDNF (R&D Systems) and 20 ng/mL GDNF (R&D Systems). Medium was replaced every other day. On day 7, neural progenitors were dissociated with Accutase and re-seeded onto poly-L-ornithine/laminin-coated tissue culture vessels to retain the initial cell density. Cells were seeded in NDM supplemented with 0.5 mM dbcAMP (Sigma-Aldrich) to promote maturation. Cells were processed for analysis between days 10 – 15.

VPR based *SNCA* overexpression

We used the previously published *SNCA* TSS2-2 sgRNA and modified F+E sgRNA backbone (19) for overexpression of *SNCA*, cloned with a human U6 promoter by overlap PCR into pGEM-Teasy (Promega) and co-transfected with the SP-dCas9-VPR vector, which was a gift from George Church (Addgene #63798). Normal alpha-synuclein (NAS) neurons were derived from NCRM-5 iPSCs, via a stable intermediate iPSC-derived neural stem cell (NSC) population (Figure S3A). On day 0, 7.5 x 10^6 NSCs were seeded onto poly-L-ornithine (Sigma)/laminin (Life Technologies)-coated T75 tissue culture flasks. On day 1, 100% medium was replaced with Neuronal Differentiation Medium consisting of Neurobasal (Life Technologies), 1X B27 supplement (Life Technologies), 1X GlutaMAX (Life Technologies), 20 ng/mL BDNF (R&D Systems) and 20 ng/mL GDNF (R&D Systems). 100% medium was replaced every other day, until day 7. On day 7, neuronal progenitors were dissociated with Accutase. 5 x 10^5 neuronal progenitors were Neon transfected with dCas9-VPR and sgRNA expression plasmids according the manufacturer's protocol, using default system settings (1400 V, 20 ms, 1 pulse). Neuronal progenitors were transfected in triplicate with 2 μg final DNA used per reaction. A CAG-driven tdTomato expression vector was used as a transfection control for all experiments. Following Neon transfection, cells were plated directly onto poly-ornithine/laminin-coated 12-well tissue culture dishes in Neuronal Differentiation Medium containing 10 μM ROCK inhibitor (Tocris Bioscience) to promote survival and 0.5 mM dbcAMP (Sigma) to promote maturation. Neurons were processed for analysis 72 hours after transfection. All RT-PCR primers are listed in Table S4.

Immunostaining

For immunostaining, cells were fixed with 4% paraformaldehyde (PFA) diluted in 1X PBS. Fixative was removed and cells rinsed three times with 1X PBS for 5 min each wash. Cells were then blocked with a solution of 0.3% Triton X-100, 5% goat serum in 1X PBS for one hour at room temperature. Blocking reagent was aspirated and primary antibodies (rabbit anti-α-synuclein, Abcam) were applied in antibody dilution buffer (0.3% Triton X-100, 1% BSA in 1X PBS) for overnight incubation at 4°C. Primary antibodies were aspirated, and cells were rinsed three times with 1X PBS for 5 min each wash. Secondary antibodies (goat anti-rabbit Alexa Fluor 488, Life Technologies, A-11034)

were applied for two hours at room temperature. Secondary antibodies were then removed and samples rinsed three times with 1X PBS for 5 min each. The cells were then mounted with VECTASHIELD Mounting Medium with DAPI (Vector Labs) and glass coverslips. Images were acquired using an EVOS FL Imaging System.

Culture and Transfection of HEK293T, BE(2)-M17 and SH-SY5Y Cells

HEK293T and SH-SY5Y cells were maintained in DMEM (Life Technologies) supplemented with 10% HyClone FBS (GE Healthcare) with complete medium replacement every 2 days. BE(2)-M17 cells were maintained in OptiMEM (Life Technologies) supplemented with 10 % HyClone FB with complete medium replacement every 2 days. Cells were passaged when reaching 70% confluence. Twenty-four hours prior to transfection HEK293T and BE(2)-M17 cells were seeded at a density of 1.3 x 10^5 cells per well to 24-well plates. HEK293T and BE(2)-M17 cells were transfected with Lipofectamine 2000 (Life Technologies) using 500 ng final DNA used per well, according to the manufacturer's instructions. SH-SY5Y cells were Neon transfected at a density of 1 x 10^6 cells and 2 μg DNA per reaction, as described above.

RNA Extraction, RT-PCR, qRT-PCR and RNA-Seq Library Preparation

Cells were lysed for RNA extraction with Qiazol lysis reagent (Qiagen) and RNA was purified on RNEasy spin columns (Qiagen). Reverse transcription was performed with SuperScript III First-Strand Synthesis SuperMix for qRT-PCR (Life Technologies), per the manufacturer's instructions. RT-PCR was performed on undiluted cDNA with Platinum PCR SuperMix (Life Technologies). RNA was diluted in nuclease-free water (Ambion) for qRT-PCR,

which was performed under standard cycling conditions with KiCqStart SYBR Green Master Mix (Sigma-Aldrich). All primers for RT-PCR and qRT-PCR are provided in Table S3.

For RNA-seq, libraries were prepared using Illumina's TruSeq Stranded mRNA HT kit (cat number RS-122-2103) from 1ug (iPSCs) or 320-400ng (neurons) total RNA, pooled and sequenced over 2 lanes of HiSeq4000 at 75b paired end.

RNA-Seq Analysis

Around 30 million reads per sample were obtained, and were quality controlled, mapped to the human genome and differential expression called using HTseq and DEseq2 (15) on the Ensembl gene set (release 82). We implemented a generalized linear model within DESeq2 to test the effect of differentiation stage (iPSC vs. neuron), genotype (AST vs AST[iso]) and interaction differentiation x genotype on gene expression. KEGG and GO pathway enrichment analysis was performed using GOseq (Young et al., 2010).

Alpha-Synuclein ELISA

Alpha-synuclein protein levels were quantified using the Human Alpha-Synuclein ELISA Kit (KHB0061, Life Technologies), according to the manufacturer's instructions. Briefly, standards and samples were diluted in Standard Diluent Buffer before loading onto Alpha-Synuclein Antibody-coated assay wells. Alpha-Synuclein Detection

Antibody was added to assay wells for three hours at room temperature. Assay wells were washed four times with 1X Wash Buffer. Anti-Rabbit IgG HRP was added to assay wells for 30 min at room temperature. Assay wells were washed four times with 1X Wash Buffer. Stabilized Chromogen was added to all wells, including chromogen blanks, for 30 min at room temperature. An equal volume of Stop Solution was added and absorbance was immediately read at 450 nm. A standard curve was generated in GraphPad Prism 6 (GraphPad Software) and used to calculate the unknown concentrations of alpha-synuclein in lysates.

Western Blotting

Protein lysates (40 μg per sample) were resolved in 15% SDS-PAGE gels and transferred to 0.45 μm pore PVDF membranes (GE Healthcare) for 2 hours at 100V in a transfer buffer containing 25 mM Tris, 200 mM glycine, and 20% (v/v) methanol. Membranes were blocked in 0.1% Tween-20 Tris-buffered saline with 5% skimmed powdered milk for 1 hour with constant agitation. Primary antibodies were diluted in blocking solution as follows: Bcl-2 1:1000 (Santa Cruz, sc-492), Beclin-1 1:500 (Santa Cruz, sc-11427), β-actin 1:5000 (Abcam, ab6276) and incubation was performed overnight at 4°C. After 4 washes in Tris-buffered saline supplemented with 0.1% Tween 20, membranes were incubated with 680 RD goat anti-rabbit IgG (Licor, 926-68071) or 800 CW goat anti-mouse IgG (Licor, 926-32210) and fluorescent signal captured with Odyssey Fc system (Li-Cor) and quantified with Image Studio 2.0 software, using β-actin as a reference protein.

Post-Mortem Brain Tissue

Human brain specimens were obtained from the Biobank Pathology unit, VU University Medical Center under approval of the ethics committee of the VU University Medical Center. Human autopsy material was obtained with informed consent for research. Formalin-fixed paraffin-embedded tissue from the mesencephalon was used from six control and five PD cases. Control cases had no known clinical history of dementia or motor disturbances, and died of causes unrelated to the central nervous system. Control and PD cases were selected based on clinical diagnosis and confirmed by neuropathological evaluation. Control cases showed no immunoreactivity for alpha-synuclein or pIRE1a in the mesencephalon. Patient characteristics including sex, age, post-mortem delay, clinical diagnosis or cause of death is shown in Table S2.

Immunohistochemistry

Sections (5 μm thick) were mounted on SuperFrost Plus tissue slides (Menzel-Gläser, Germany) and deparaffinized. Subsequently, sections were immersed in 0.3% H_2O_2 in methanol for 30 min to quench endogenous peroxidase activity. Sections were treated in 10 mM pH 6.0 citrate buffer heated by microwave during 10 min for antigen retrieval. Primary antibodies were dissolved in Normal Antibody Diluent (Immunologic, Duiven, The Netherlands) and applied overnight at 4°C. Rabbit anti-pIRE1a (pSer724, Novus Biologicals, Littleton, CO, USA) was diluted 1:10,000 and mouse anti-alpha-synuclein (clone LB509, Zymed Laboratories, San Francisco, CA) was used at a 1:200 dilution. Between incubation steps, sections were rinsed with phosphate buffered saline (PBS, pH 7.4). As secondary step, sections were incubated with EnVision detection system (goat anti-mouse/rabbit horseradish peroxidase, DAKO) for 30 minutes at room temperature. Color was developed using 3-amino-9-ethyl-carbazole (AEC, Zymed, San Francisco, CA) and nuclei were stained with haematoxylin. Immunohistochemical evaluation was performed on the substantia

nigra pars compacta and pars reticulata at the level of the third cranial nerve. The immunoreactivity score ranged from

0 to 2, with 0 indicating no, 1 moderate, and 2 strong immunoreactivity of the relevant antibody in the studied cells. The IHC score for each case was an average of at least four microscopic fields (magnification 10X).

To determine the colocalization of pIRE1a with alpha-synuclein, double-immunohistochemistry was performed on two PD cases. Sections were immersed in 0.3% H_2O_2 in methanol for 30 min to quench endogenous peroxidase activity. Sections were treated in 10 mM pH 6.0 citrate buffer heated by microwave during 10 min for antigen retrieval. Subsequently, sections were co-incubated with rabbit anti-pIRE1a (dilution 1:10,000) and mouse anti-alpha-synuclein (dilution 1:200, clone LB509, Zymed Laboratories, San Francisco, CA) diluted in normal antibody diluent overnight at 4°C. Sections were washed with PBS and co-incubated with EnVision (goat anti-rabbit HRP, DAKO) and alkaline phosphatase conjugated goat anti-mouse IgG (dilution 1:200, SouthernBiotech, Birmingham AL, USA) for 30 min. Sections were washed and colors were developed with AEC and subsequently with Fast Blue BB Base (Sigma, St. Louis, MO). Sections were counterstained with haematoxylin and mounted using Aquamount (BDH, Poole, England). The Nuance spectral imaging system (CRi, Woburn, MA) was used for the analysis of double-stained specimens. Spectral imaging unmixes colors based on their spectral characteristics, enabling visualization of the different reaction products. Spectral imaging data cubes were taken from 460-660 nm at 10 nm intervals and analyzed with the Nuance software. Spectral libraries of single-red (AEC), single-blue (Fast Blue BB Base), neuromelanin and haematoxylin were obtained from control slides. The resulting library was applied to the double stained slides and the different reaction products were then spectrally unmixed into individual black-and-white images, representing the localization of each of the reaction products, and reverted to fluorescence-like images composed of pseudo-colors using the Nuance software.

Statistical Methods

Results of qRT-PCR experiments represent technical triplicates of biological triplicates, and results of alpha-synuclein ELISA represent technical duplicates of biological triplicates. Levene's homogeneity test was used to evaluate the null hypothesis that population variances were equal. Statistical significance was determined by one-way ANOVA with post-hoc Bonferonni where samples met the homogeneity of variances assumption or Games-Howell where samples did not meet the homogeneity of variances assumption.

SUPPLEMENTARY REFERENCES

Chambers, S.M., Fasano, C.A., Papapetrou, E.P., Tomishima, M., Sadelain, M., and Studer, L. (2009). Highly efficient neural conversion of human ES and iPS cells by dual inhibition of SMAD signaling. Nature biotechnology *27*, 275-280.

Young, M.D., Wakefield, M.J., Smyth, G.K., Oshlack, A. (2010) Gene ontology analysis for RNA-seq: accounting for selection bias. Genome Biol. *11*, R14.